Peptide Nanoconjugation

DOI: 10.1002/anie.201209662

# Orientation-Controlled Conjugation of Haloalkane Dehalogenase Fused Homing Peptides to Multifunctional Nanoparticles for the Specific Recognition of Cancer Cells**

*Serena Mazzucchelli,* Miriam Colombo, Paolo Verderio, Ewa Rozek, Francesco Andreata, Elisabetta Galbiati, Paolo Tortora, Fabio Corsi, and Davide Prosperi**

Multifunctional nanoparticles (MNPs) that combine unique superparamagnetic properties and fluorescence emission are promising bimodal tracers for the noninvasive diagnosis of malignant cells both in vitro and in vivo.[1–4] The selective recognition of specific cancer cells impacts diagnostic sensitivity, and it can be accomplished by the functionalization of MNPs with molecules that have a high affinity for specific membrane receptors.[5–7] However, the mode in which individual homing ligands are immobilized at the interface between the inorganic core and the biological environment, may strongly affect the actual targeting efficiency of the nanoconjugate.[8–10] A generally underestimated concern is the molecular organization at the nanoscale, which is a relevant consideration for protein ligands and is even crucial when short peptides are used. To optimize the recognition by a specific biological receptor, the immobilized peptide needs to be stably ligated to the nanoparticle but sufficiently mobile to interact with the receptor. Indeed, peptides tend to bind to the surface of an MNP through hydrophobic residues, which is promoted by entropic stabilization and electrostatic interactions and exploits polar and dissociated groups in the peptide sequence .[11] This often results in a loss or reduction of delivery efficiency and, more importantly, of target selectivity. For this reason, the development of effective and reliable strategies to afford ordered ligand orientation on the nanoparticle surface has attracted a lot of interest in nanomedicine.[8,12,13] Several approaches have been explored to control ligand positioning, including conjugation mediated by affinity tags inserted into the protein primary sequence,[14,15] oriented immobilization on MNPs driven by recombinant protein linkers,[16,17] and site-specific chemo-selective ligation.[18,19] Recently, we have proposed a novel approach that relies on engineered proteins consisting of a receptor-targeting domain genetically fused with a nanoparticle-capture domain, in which the capture module should be an enzyme capable of irreversibly reacting with a suicide inhibitor covalently anchored on MNP. As a proof of concept, we have immobilized an scFv antibody fused to a SNAP tag onto MNPs.[20] The same approach was exploited for ligand functionalization of pegylated capsules.[21] In principle, this bimodular orthogonal bioreaction could present two important advantages when the homing ligand is a short peptide (i.e., 5–30 aa): 1) the peptide is separated from the nanoparticle surface by a protein spacer, which prevents undesired interactions and thus optimizes the ligand availability for molecular recognition; 2) the introduction of globular proteins (i.e., the reacting enzyme) enhances the solubility of the nanoconstruct.

Haloalkane dehalogenase (HALO) from *Rhodococcus rhodochrous* forms an ester bond between aspartate 106 in the enzyme and the substrate, concomitantly removing halides from aliphatic hydrocarbons. Substitution of His272 with a phenylalanine prevents the substrate release, which usually occurs in native HALO, and thus an stable bond can be formed between HALO and an alkyl conjugate (Figure 1).[22] Hence, we reasoned that a chloroalkane linker could be a good candidate to mediate the covalent, oriented immobilization on MNP of homing peptides genetically fused with HALO.

We designed a bimodular genetic fusion (HALO–U11) comprising a small peptide of 11 amino acids (U11) that has a high affinity for urokinase plasminogen activator receptor (uPAR), which is overexpressed in several metastasizing tumors, as a targeting module, and HALO, as an MNP capture module (Figure 1). We demonstrate the utility of this method for peptide nanoconjugation and cellular imaging by evaluating the capability of MNP covalently bound with HALO–U11 to specifically recognize uPAR-positive cancer cells. UPAR is up-regulated in a broad range of cancer cell types and tumor-associated stromal cells, and mediates various biological processes at the cell surface, including plasminogen activation, extracellular matrix invasion, cell adhesion, and metastasis.[23] U11 is believed to be the primary

[*] Dr. M. Colombo, P. Verderio, E. Rozek, F. Andreata, E. Galbiati, Prof. P. Tortora, Dr. D. Prosperi
NanoBioLab, Dipartimento di Biotecnologie e Bioscienze
Università di Milano Bicocca
Piazza della Scienza 2, 20126 Milano (Italy)
E-mail: davide.prosperi@unimib.it
Homepage: http://www.nanobiolab.btbs.unimib.it
Dr. D. Prosperi
Labion, Polo Tecnologico, Fondazione Don Gnocchi IRCCS-ONLUS
Via Capecelatro 66, 20148 Milano (Italy)
Dr. S. Mazzucchelli, Dr. M. Colombo, Prof. F. Corsi
Dipartimento di Scienze Biomediche e Cliniche "Luigi Sacco"
Università di Milano, Ospedale L. Sacco
Via G.B. Grassi 74, 20157 Milano (Italy)
E-mail: serena.mazzucchelli@gmail.com

[**] M.C. acknowledges the research fellowships of CMENA. This work was partly supported by Fondazione Regionale per la Ricerca Biomedica (FRRB), NanoMeDia Project, and Fondazione "Romeo ed Enrica Invernizzi".

Supporting information for this article is available on the WWW under http://dx.doi.org/10.1002/anie.201209662.

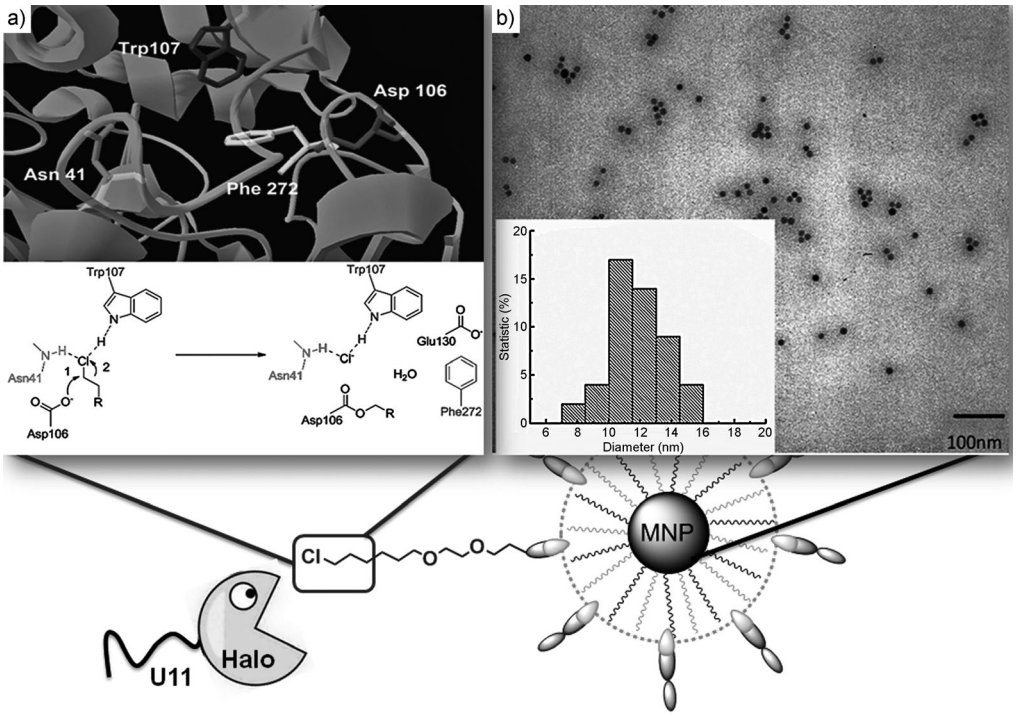


***Figure 1.*** A) Schematic representation of a HALO-conjugated multifunctional nanoparticle (**MNP-H**). a) Interaction of haloalkane anchor ligand with the genetically modified HALO binding site. b) TEM image of **MNP-H11** (inset: size distribution of the nanoparticles).

uPAR binding motif with a dissociation constant of 1.3–1.4 μM.[24,25]

The HALO sequence was modified by selective mutagenesis of the native protein (see the Supporting Information).[22] Moreover, *SalI* and *XhoI* restriction sites were inserted at the 5′- and 3′-positions, respectively, and the modified gene was cloned in a pGEX-6-P-1 vector to express HALO fused with glutathione *S*-transferase (GST). HALO was expressed in BL21(DE3) codon plus *E. coli* strain. After induction with isopropyl β-D-1-tiogalactopiranoside (IPTG), cells were collected and disrupted, HALO was isolated from the crude extract by using a glutathione–sepharose column and eluted by PreScission protease cleavage (1 mg $L^{-1}$ yield). Purified fractions showed an excellent degree of purity, despite the presence of a residual GST contaminant (see the Supporting Information, Figure S3).

The anchor ligand **L1** containing a chlorohexane moiety, which is reactive toward the HALO binding site, was synthesized in three steps from simple precursors (see the Supporting Information, Scheme S1). Magnetite nanoparticles with narrow size distribution (10.1 ± 1.3 nm, **MNP0**) capped by oleate surfactant were obtained by solvothermal decomposition in organic solvents,[26] and they were transferred to the water phase by coating them with an amphiphilic polymer (PMA) in sodium borate buffer (pH 12).[20,27] The resulting PMA-coated nanoparticles (**MNP1**) were superparamagnetic and exhibited excellent solubility in aqueous media. Amino groups were introduced on **MNP1** by using a homobifunctional linker (2,2-(ethylenedioxy)bisethylamine; EDBE) to give **MNP2. L1** was linked to the amines on the polymer envelope through nucleophilic addition to the *p*-nitrophenyl carbonate group by incubation overnight at 4 °C (**MNP3**, Scheme 1). **MNP3** were characterized by dynamic light scattering (DLS), and exhibited a mean hydrodynamic size of 40.1 ± 2.7 nm in PBS (5 μg $mL^{-1}$, pH 7.4) with a zeta potential of −28.5 ± 3.0 mV. **MNP3** was very stable in PBS buffer and formed a dark transparent solution.

The optimal conditions for the conjugation of the fusion protein with **L1** on MNP was determined by varying several experimental parameters, including the protein/nanoparticle ratio, time, temperature, and incubation buffer (see the Supporting Information,

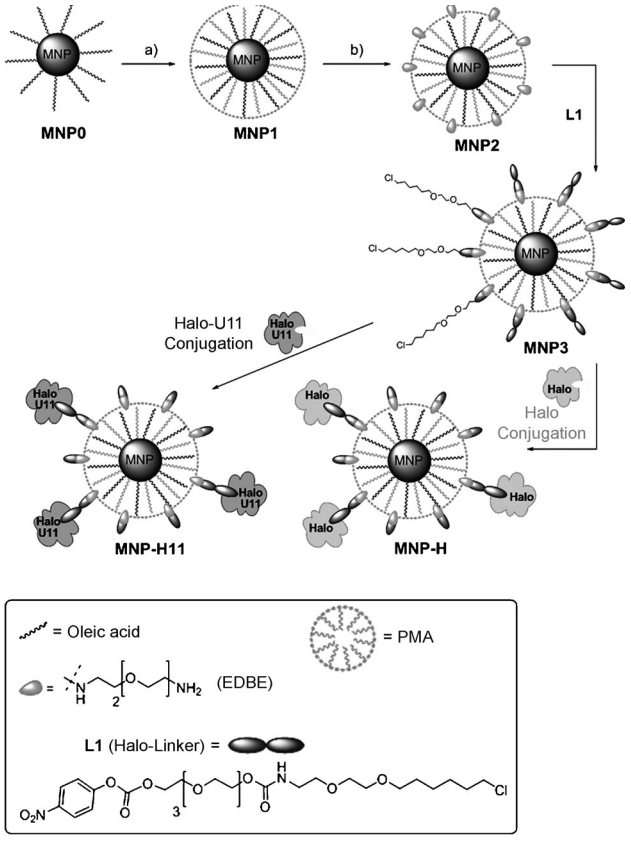


***Scheme 1.*** Synthesis of HALO-functionalized multifunctional nanoparticles (**MNP-H** and **MNP-H11**). a) PMA, SBB, pH 12; b) EDBE, EDC, water. EDBE = 2,2-(ethylenedioxy)bisethylamine, EDC = *N*-(3-dimethylaminopropyl)-*N*′-ethylcarbodiimide hydrochloride, PMA = amphiphilic polymer, SBB = sodium borate buffer.

  

Table S1). HALO-functionalized MNP (**MNP-H**) were obtained by treating purified fluoresceine isothiocyanate (FITC) labeled HALO with **MNP3** in a 1:1 ratio (w/w) in PBS, pH 7.4 (Scheme 1). After 1 h incubation at 25 °C, unconjugated HALO was removed by centrifuging the mixture in amicon YM-100 tubes and the concentrated nanoparticles were further reacted with α-methoxy-ω-amino-PEG (2 kDa, $mPEG_{2k}$-$NH_2$), after activation of the carboxylate groups of the polymer by EDC, to minimize possible nonspecific adsorption. The nanoparticles were then washed three times with PBS. The amount of unreacted dye-labeled HALO was fluorometrically measured after first establishing a standard calibration curve, which provided the number of HALO molecules attached to each nanoparticle. We determined the presence of an average of about 5 HALO molecules per **MNP-H**. DLS analysis showed an increment in the hydrodynamic size upon conjugation ($62.9 \pm 7.2$ nm), consistent with the attachment of protein molecules, and the nanoparticles were stable owing to a negative zeta potential of $-32.3 \pm 0.4$ mV. To assess whether the conjugation occurred specifically to **L1**, HALO was incubated with **MNP2**, as a control. No binding, within the fluorescence assay sensitivity, occurred to nanoparticles in the absence of **L1**, thus demonstrating that HALO immobilization on the nanoparticles was indeed mediated by ligand interaction with the active site of the enzyme. Moreover, sodium dodecyl sulphate–polyacrylamide gel electrophoresis (SDS-PAGE) (Figure S4) showed that, whereas protein incubated with **MNP2** was able to migrate upon the application of a current, no HALO molecules were released from **MNP-H**.

After preliminary assessment of the efficiency of the HALO conjugation, a HALO capture module was engineered by the introduction of a targeting element that consists of the 11 amino acid sequence VSNKYFSNIHW (U11) involved in uPAR recognition, through a C-terminal insertion of a GGGGSGGGG loop, which provides sufficient freedom to U11 (Figure S5). HALO–U11 fusion protein was produced in BL21(DE3) *E. coli* and purified by using the same procedure described above for HALO, and then HALO–U11 was reacted with FITC-labeled MNP3 by using the conjugation protocol illustrated in Scheme 1, to give **MNP-H11** (size $= 67.6 \pm 3.1$ nm, zeta potential $= -27.8 \pm 2.6$ mV). In this case, the fluorescent label was covalently incorporated inside the polymer layer to avoid contact of the dye with the external environment, which could affect the nanoparticle affinity for cellular receptors.

U937 cell lines were selected as the cellular model to assess the targeting efficiency of **MNP-H11**, because these cancer cells are available both as uPAR-positive (U937_13) and as uPAR-negative (U937_10). The only difference between them was the membrane expression of a U11-specific receptor. U937_13 cell lines were first treated in parallel with dye-labeled **MNP2** and HALO to evaluate nonspecific interactions of the pegylated nanoparticles and of the capture protein, respectively, with $uPAR^+$ cells. In both cases, no evidence of cell labeling was detected by flow cytometry (see the Supporting Information, Figure S8). To assess the influence of the controlled orientation of ligand presented HALO–U11, MNP were also directly conjugated with U11 peptide (4–6 molecules per MNP) by introducing a Cys residue at the C-terminal (**MNP-U11**). **MNP-H11** and **MNP-U11** were each incubated for 1 h with U937_13 and with U937_10 (control) cancer cells at two different concentrations (20 μg mL$^{-1}$ and 100 μg mL$^{-1}$). Flow cytometry performed on the U937_13 cells treated with **MNP-H11** evidenced a twentyfold increase in the percentage of cells in the positive region compared to **MNP-U11**-treated cells (Figure 2). Quite surprisingly, **MNP-U11** were not able to

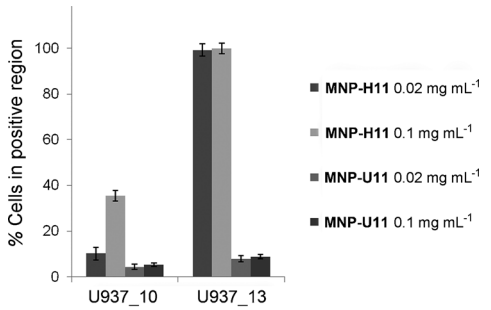


***Figure 2.*** **MNP-H11** and **MNP-U11** binding specificity to uPAR. U937 $uPAR^+$ (U937_13) and $uPAR^-$ (U937_10) cells were incubated at 37 °C with **MNP-H11** and **MNP-U11** at two different concentrations (0.02 mg mL$^{-1}$ and 0.1 mg mL$^{-1}$) for 1 h and then processed for flow cytometry. Untreated cells were used to set the positive region. Data are expressed as means ± standard error (SE) of three individual experiments.

bind $uPAR^+$ cells any more than to $uPAR^-$, probably owing to a low availability of the short peptides for recognition. U937_10 cells remained mostly unlabeled after **MNP-H11** treatment, even at 100 μg mL$^{-1}$. These results demonstrated that the controlled peptide orientation is crucial for optimal target specific recognition, as **MNP-H11** were captured selectively by uPAR-expressing U937_13 cells.

The specificity of the binding between **MNP-H11** and uPAR was confirmed by confocal laser scanning microscopy. U937_13 and U937_10 cells (CTRL-) were treated in parallel with **MNP-H11** (100 μg mL$^{-1}$) for 1 h at 37 °C. As a uPAR expression control, U937_13 cells were immunodecorated with anti-uPAR antibody (CTRL +). **MNP-H11** were localized in the proximity of the cell membrane and inside the cytoplasm of $uPAR^+$ cells only, showing a uPAR recognition pattern similar to the positive control; this finding confirmed that **MNP-H11** adhesion to the cell membrane and internalization were actually mediated by specific interactions with the U11 peptide (Figure 3). Finally, cell-death experiments performed on U937_13 cells after 24 h incubation with **MNP-H11** at 20 μg mL$^{-1}$ and 100 μg mL$^{-1}$, suggested that **MNP-H11** were nontoxic within this range of concentrations; this finding is significant for in vitro and in vivo applications (Figure 4).

In summary, we have established a new bimodular strategy for controlled peptide positioning on multifunctional nanoparticles. The advantages of our approach are: 1) the peptide was produced fused to a capture domain (HALO) by recombinant expression, which afforded the active targeting ligand in high purity and avoided chemical synthesis and

  

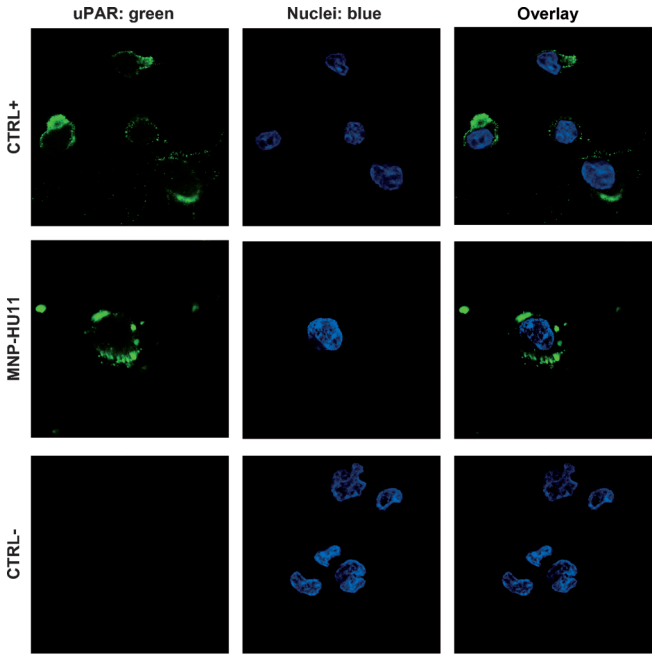


***Figure 3.*** Confocal microscopy images of U937 uPAR$^+$ and uPAR$^-$ (CTRL−) cells, incubated for 1 h at 37 °C with **MNP-H11** (0.1 μg mL$^{-1}$, green). As a positive uPAR-expression control (CTRL+), U937 uPAR$^+$ cells were immunodecorated with anti-uPAR primary antibody, revealed with an anti-mouse secondary antibody conjugated with Alexa fluor 488 (Invitrogen). Nuclei were stained with 4′,6-diamidino-2-phenylindole (DAPI). Scale bar: 10 μm.

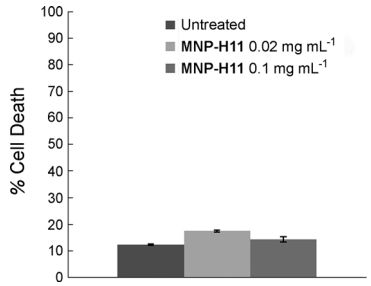


***Figure 4.*** Cell-death assay. U937 uPAR$^+$ cells were treated with **MNP-H11** (0.02 mg mL$^{-1}$ and 0.1 mg mL$^{-1}$) for 24 h (light and dark grey, respectively). Cell death was assessed by measuring the exposure of Annexin V and the incorporation of 7-aminoactinomycin D and evaluated by flow cytometry. An untreated sample is shown as negative control. All results are expressed as means ± SE of five individual experiments.

purification; 2) the recombinant peptide was designed to achieve an efficient covalent conjugation to MNP functionalized with simple linkers in an orientation-controlled manner; 3) selective immobilization was accomplished by an enzymatic biorecognition event, which prevented nonspecific adsorption provided that MNP were properly pegylated. In this way, highly active **MNP-H11** were engineered, and proved to be very effective in selectively targeting uPAR-positive cancer cells. This method is simple and versatile and offers a new solution for the covalent immobilization on MNP of active homing ligands directed to a broad spectrum of specific biomarkers; these nanoparticles can be exploited for the development of nanoparticle-based diagnosis and treatments of human malignancies.

Received: December 3, 2012
Revised: January 1, 2012
Published online: February 5, 2013

**Keywords:** bioconjugation · cell targeting · peptides · nanoparticles · receptors

[1] K. Park, S. Lee, E. Kang, K. Kim, K. Choi, I. C. Kwon, *Adv. Funct. Mater.* **2009**, *19*, 1553 – 1566.
[2] J.-H. Lee, Y.-M. Huh, Y.-w. Jun, J.-w. Seo, J.-t. Jang, H.-T. Song, S. Kim, E.-J. Cho, H.-G. Yoon, J.-S. Suh, J. Cheon, *Nat. Med.* **2007**, *13*, 95 – 99.
[3] J. Kim, S. Park, J. E. Lee, S. M. Jin, J. H. Lee, I. S. Lee, I. Yang, J.-S. Kim, S. K. Kim, M.-H. Cho, T. Hyeon, *Angew. Chem.* **2006**, *118*, 7918 – 7922; *Angew. Chem. Int. Ed.* **2006**, *45*, 7754 – 7758.
[4] F. Corsi, L. Fiandra, C. De Palma, M. Colombo, S. Mazzucchelli, P. Verderio, R. Allevi, A. Tosoni, M. Nebuloni, E. Clementi, D. Prosperi, *ACS Nano* **2011**, *5*, 6383 – 6393.
[5] M. Lewin, N. Carlesso, C.-H. Tung, X.-W. Tang, D. Cory, D. T. Scadden, R. Weissleder, *Nat. Biotechnol.* **2000**, *18*, 410 – 414.
[6] N. T. K. Thanh, L. A. W. Green, *Nano Today* **2010**, *5*, 213 – 230.
[7] D. Simberg, T. Duza, J. H. Park, M. Essler, J. Pilch, L. Zhang, A. M. Derfus, M. Yang, R. M. Hoffman, S. Bhatia, M. J. Sailor, E. Ruoslahti, *Proc. Natl. Acad. Sci. USA* **2010**, *104*, 932 – 936.
[8] E. Occhipinti, P. Verderio, A. Natalello, E. Galbiati, M. Colombo, S. Mazzucchelli, A. Salvadè, P. Tortora, S. Maria Doglia, D. Prosperi, *Nanoscale* **2011**, *3*, 387 – 390.
[9] M. E. Aubin-Tam, K. Hamad-Schifferli, *Biomed. Mater.* **2008**, *3*, 034001.
[10] K. Boeneman, J. R. Deschamps, S. Buckhout-White, D. E. Prasuhn, J. B. Blanco-Canosa, P. E. Dawson, M. H. Stewart, K. Susumu, E. R. Goldman, M. Ancona, I. L. Medintz, *ACS Nano* **2010**, *4*, 7253 – 7266.
[11] K. H. Lee, F. M. Ytreberg, *Entropy* **2012**, *14*, 630 – 641.
[12] I. Medintz, *Nat. Mater.* **2006**, *5*, 842.
[13] W. R. Algar, D. E. Prasuhn, M. H. Stewart, T. L. Jennings, J. B. Blanco-Canosa, P. E. Dawson, I. L. Medintz, *Bioconjugate Chem.* **2011**, *22*, 825 – 858.
[14] C. Xu, K. Xu, H. Gu, X. Zhong, Z. Guo, R. Zheng, X. Zhang, B. Xu, *J. Am. Chem. Soc.* **2004**, *126*, 3392 – 3393.
[15] M. J. C. Long, Y. Pan, H.-C. Lin, L. Hedstrom, B. Xu, *J. Am. Chem. Soc.* **2011**, *133*, 10006 – 10009.
[16] S. Mazzucchelli, M. Colombo, C. De Palma, A. Salvadè, P. Verderio, M. D. Coghi, E. Clementi, P. Tortora, F. Corsi, D. Prosperi, *ACS Nano* **2010**, *10*, 5693 – 5702.
[17] I. García, J. Gallo, N. Genicio, D. Padro, S. Penadés, *Bioconjugate Chem.* **2011**, *22*, 264 – 273.
[18] C.-C. Yu, P.-C. Lin, C.-C. Lin, *Chem. Commun.* **2008**, 1308 – 1310.
[19] M. Colombo, S. Sommaruga, S. Mazzucchelli, l. Polito, P. Verderio, P. Galeffi, F. Corsi, P. Tortora, D. Prosperi, *Angew. Chem.* **2012**, *124*, 511 – 514; *Angew. Chem. Int. Ed.* **2012**, *51*, 496 – 499.
[20] M. Colombo, S. Mazzucchelli, J. M. Montenegro, E. Galbiati, F. Corsi, W. J. Parak, D. Prosperi, *Small* **2012**, *8*, 1492 – 1497.
[21] M. K. M. Leung, C. E. Hagemeyer, A. P. R. Johnston, C. Gonzales, M. M. J. Kamphuis, K. Ardipradja, G. K. Such, K. Peter, F. Caruso, *Angew. Chem.* **2012**, *124*, 7244 – 7248; *Angew. Chem. Int. Ed.* **2012**, *51*, 7132 – 7136.

[22] G. V. Los, L. P. Encell, M. G. McDougall, D. D. Hartzell, N. Karassina, C. Zimprich, M. G. Wood, R. Learish, R. Friedman Ohana, M. Urh, et al., *ACS Chem. Biol.* **2008**, *3*, 373 – 382.
[23] F. Blasi, N. Sidenius, *FEBS Lett.* **2010**, *584*, 1923 – 1930.
[24] Q. Huai, A. P. Mazar, A. Kuo, G. C. Parry, D. E. Shaw, J. Callahan, Y. Li, C. Yuan, C. Bian, L. Chen, et al., *Science* **2006**, *311*, 656 – 659.
[25] M. Wang, D. W. P. M. Löwik, A. D. Miller, M. Thanou, *Bioconjugate Chem.* **2009**, *20*, 32 – 40.
[26] J. Park, K. An, Y. Hwang, J.-G. Park, H.-J. Noh, J.-Y. Kim, J.-H. Park, N.-M. Hwang, T. Hyeon, *Nat. Mater.* **2004**, *3*, 891 – 895.
[27] C.-A. J. Lin, R. A. Sperling, J. K. Li, T.-Y. Yang, P.-Y. Li, M. Zanella, W. H. Chang, W. J. Parak, *Small* **2008**, *4*, 334 – 341.

  